Adaptive optics for the 6.5 m MMT

M. Lloyd-Hart, F. Wildi, H. Martin, P. McGuire, M. Kenworthy, R. Johnson, B. Fitz-Patrick, G. Angeli, S. Miller, R. Angel

Center for Astronomical Adaptive Optics, University of Arizona, Tucson, AZ 85721

ABSTRACT

The adaptive optics system for the 6.5 m MMT conversion telescope will be the first to compensate the aberrated wavefront at the telescope's secondary mirror. This approach has unique advantages in terms of optical simplicity, high throughput and low emissivity. We report here the present state of construction, and the results of static and dynamic performance tests of the Cassegrain optical package.

1. INTRODUCTION

The MMT adaptive optics system is conceived as an integral part of the 6.5 m telescope. Compensation of atmospheric aberration will be done to high order at a deformable secondary mirror,[1] giving a corrected f/15 Cassegrain focus. Wavefront sensing will be done in an opto-mechanical package bolted to the instrument rotator. The lower side of the package presents a flange centered on the corrected beam to which a variety of instruments may be mounted.

A number of technological challenges have had to be addressed in the design and construction of the AO system. Firstly, we have had to learn how to make a large, very thin piece of curved glass with 80 μm of asphericity.[2] The polishing and figuring of the asphere have now been completed, and after correction of low-order fixed aberration by the actuators, it is expected to achieve 19 nm rms surface quality.

Control of the shape of such a large piece of glass at the level required to preserve the near infrared diffraction limit is non-trivial. Using a sub-scale prototype, we have recently demonstrated the ability to track realistic turbulence with excellent accuracy.[3] We rely on purely passive techniques to prevent excitation of the glass membrane in its many natural resonant modes.

Tests of the deformable mirror are complicated by its convex shape. In the lab, a frame holds the optics to simulate the telescope optical path. By placing a full-size doublet lens immediately in front of the secondary, the light path from the primary can be mimicked. Using this assembly, we have begun static and dynamic tests of the Shack-Hartmann wavefront sensor (WFS) and its fore-optics, which together reside in the Cassegrain package (the "top box"). By comparing the output of the WFS to a simultaneous measurement of the wavefront exiting the system by an integral phase shifting interferometer, the WFS has been very well calibrated. In addition, we have used a prototype WFS at the prime focus of the telescope[4] for a first look at the character of the turbulence which the AO system will encounter.

In parallel, we are proceeding with the construction of a 50 cm refractive telescope to launch a sodium laser guide beacon. The beam will be routed up the side of the MMT, and launched from behind the secondary mirror. The main assemblies, including the three large glass elements, are currently in fabrication.

In the meantime, services and support facilities such as cooling for the secondary and Cassegrain packages and data routing at the telescope are in progress, and a big software effort is underway to provide a single-user GUI through which all system functions will be operated.

2. STATUS OF THE 6.5 m TELESCOPE

The new 6.5 m telescope has been constructed[5] inside the building once occupied by the Multiple Mirror Telescope (MMT). Most of the old facility has been recycled, but the new telescope has significantly more light collecting power, and better optical quality.

At the present time, the primary mirror has been aluminized (a process done in situ), and work is underway to characterize the

In *Adaptive Optical Systems Technology*, Peter L. Wizinowich, Editor,
Proceedings of SPIE Vol. 4007 (2000) • 0277-786X/00/$15.00

active primary mirror supports, and to implement the active mirror cooling system. No secondary mirrors have yet been installed, but preliminary data from the prime focus (figure 1) indicate that the telescope and site are of excellent quality, delivering images of 0.5 arcsec quality.[6]

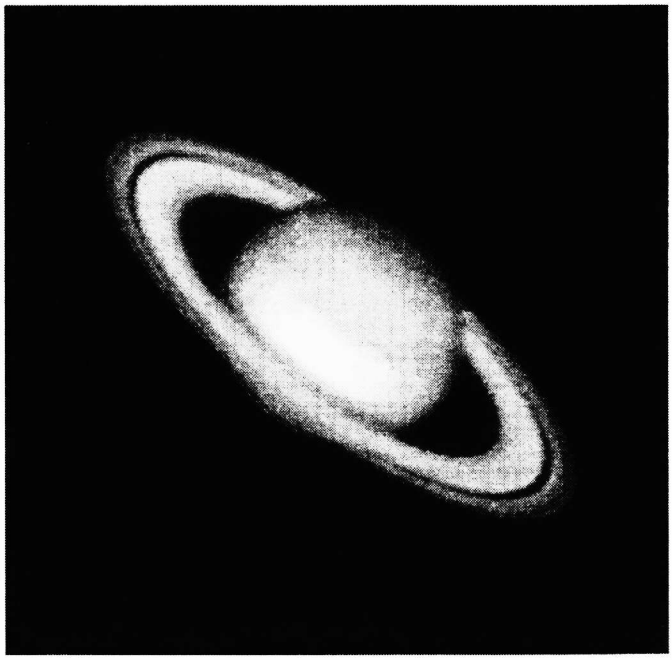

Figure 1. Image of Saturn taken on October 28 1999 with the new MMT at prime focus, with coma correcting foreoptics. The field-of-view is $41'' \times 41''$.

3. ADAPTIVE OPTICS SYSTEM DEVELOPMENT

After reflection from the primary mirror, aberrations in the wavefront are corrected at the deformable secondary, and the compensated beam is reflected to the Cassegrain focus. Here, a dichroic beamsplitter allows infrared light > 1 micron to pass into the ARIES high-resolution infrared imager and echelle spectrograph.[7] Visible light is reflected upward into the top box for wavefront sensing.

3.1. Lab Test System

In February 1999, a test-optics tower was built at the Mirror Laboratory. This tower (otherwise known as the shimmulator) serves as a simulator environment for the complete system with phase aberration provided by spinning turbulence plates. The tower, top box, and the cast optics bed are pictured in Figure 2.

The shimmulator consists of a 4 ton steel structure to support the adaptive secondary, two large lenses, two large fold-flat mirrors, and the top box. It stands about 7 meters off the ground and is isolated from vibrations by air suspension. The entire MMT telescope optics is simulated by employing two 70 cm diameter spherical lenses immediately below the adaptive secondary, and a corrective computer generated hologram (CGH) near the yellow HeNe laser source in the top box. The initial optical alignment of the shimmulator, employing surveying tools (a theodolite and alignment telescope), was completed in April 1999.

In order to test the shimmulator prior to delivery of the adaptive secondary, a 'dummy' secondary with a rigid spherical surface was made at the Mirror Lab. A fiber-fed phase-shifting interferometer (PSI) was installed as an integral part of the top box, allowing precise characterization of the system's wavefront error. The PSI is essential both for alignment of the rigid optics, and to calibrate the wavefront sensor camera and wavefront reconstructor algorithms. Final alignment of the entire system was completed in July 1999, with residual wavefront aberration less than 1 wave rms (figure 3), dominated by trefoil from the dummy secondary's three-point support.

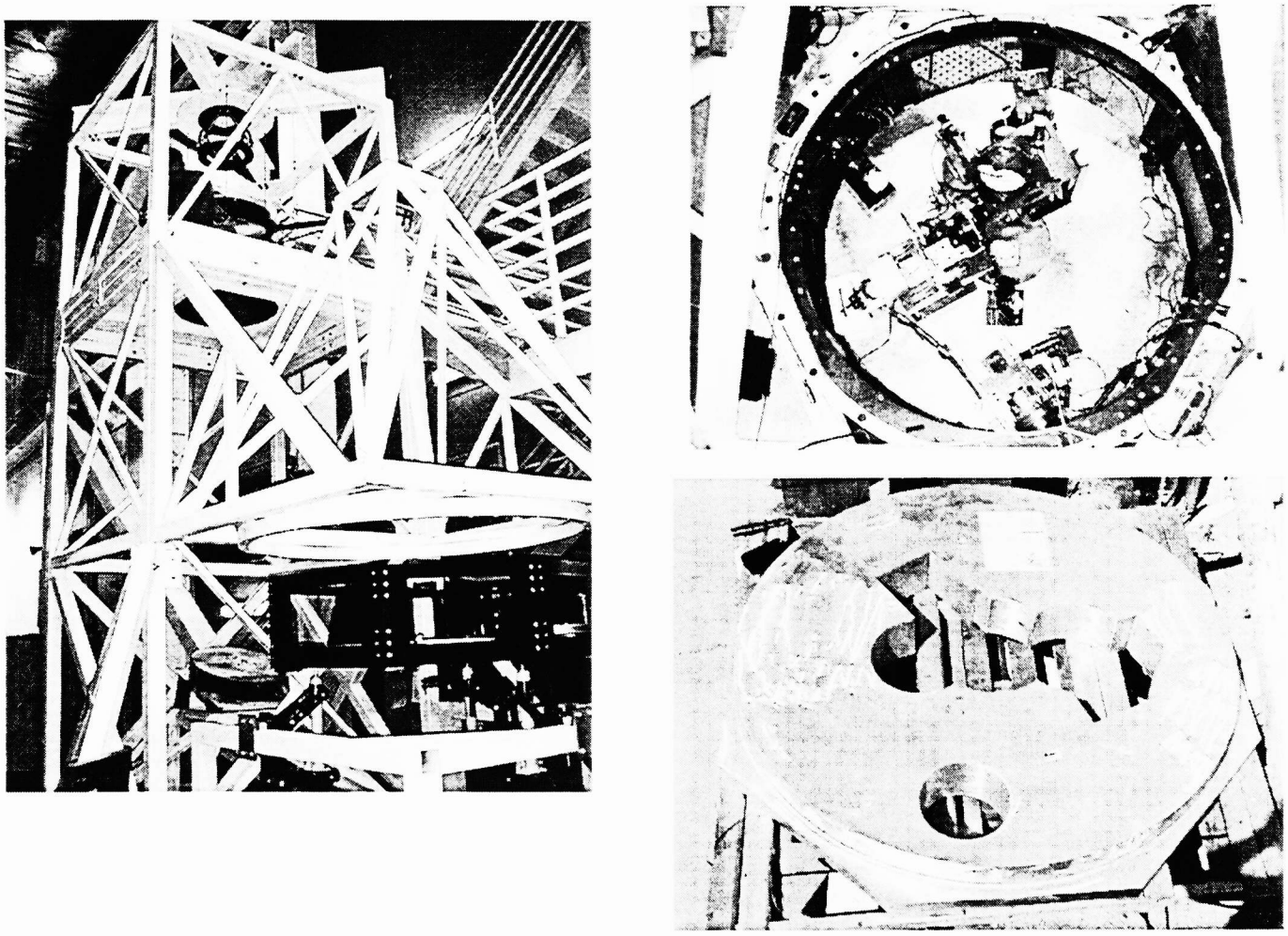

Figure 2. Shimmulator mechanical structure (left), showing the large fold flats and the unmounted top box on its handling cart. The top box (top right) is normally raised from its handling cart and mounted to the dummy rotator ring. (Lower right) the cast aluminum optics bed which forms the floor of the top box. The cutouts are designed to accommodate existing instruments.

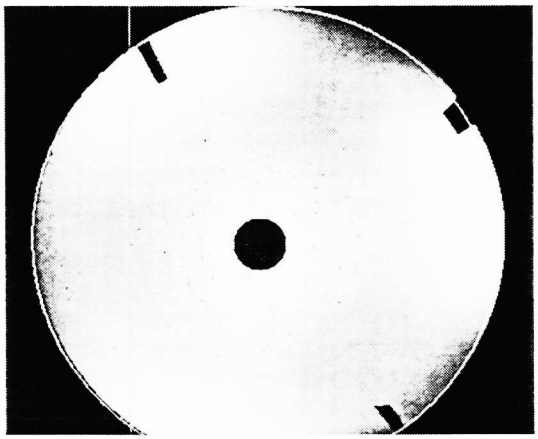

Figure 3. The optical aberration map for the Shimmulator optics and the solid dummy secondary, measured with a fiber-fed phase-shifting interferometer.

Top box optics and the WFS were installed in August 1999. Because of the need both to rotate the WFS camera (to track field rotation), and to translate it (to track changes in the distance to the sodium layer), no fewer than four optical and mechanical axes must coincide to tight tolerances when installing the WFS. Two rotating turbulence plates have also been added (figure 4). These are placed in the light path as it diverges from a pinhole source. By varying the speed of rotation, and the position along the z-axis, both r_0 and τ_0 can be infinitely varied over the range expected at the telescope.

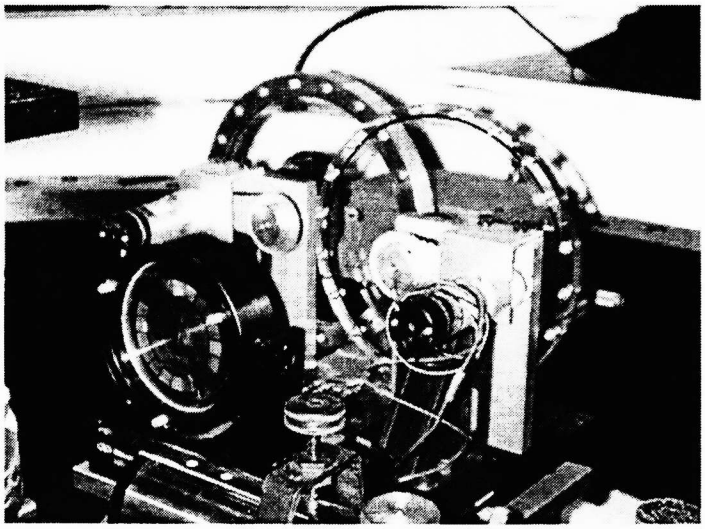

Figure 4. Arrangement of two spinning phase plates in the optical path of the shimmulator. They are machined acrylic plates filled with index-matching oil. At lower left is the computer generated hologram that removes spherical aberration from the shimmulator optics.

At present, the shimmulator has been partially disassembled as the dummy secondary is removed. In its place, we are installing the final aspheric shell, still attached to the rigid blocking body used to support the piece during grinding and polishing. When the shimmulator is reassembled, final calibration measurements will be made for both the WFS and the electro-mechanical alignment systems. The asphere will then be detached from its blocking body for integration with the adaptive secondary support and control system now nearing completion in Italy.

3.2. Wavefront Sensor

The WFS is Shack-Hartmann sensor with a MAT (EEV) CCD39a device. The lenslet array, which has lenslets on a pitch commensurate with the CCD pixels, is bonded directly to the CCD package. By chance, the CTE of gray alumina (the material of the CCD package) and the CTE of the lenslet array substrate, BK7, match to $< 1\times10^{-6}$. There is therefore no problem with bonding the two materials together and then cooling the package by 90 °C, as is done in the WFS's thermoelectrically cooled head.

The transfer curve of the camera has been measured (figure 5), and has been found to match predictions based upon prior measurements of the inter-pixel cross-talk caused by charge diffusion. The gradient of the average transfer curve at the origin (that is, the WFS's closed-loop sensitivity) is rather high, thanks to the intimate gluing of the lenslet array and the CCD chip. Read noise is also excellent, measured at 3.5 – 4.0 electrons at the full frame rate of 750 Hz.

3.2.1. Prime focus measurements

Knowing the statistical behavior of the optical wavefront as perturbed by the atmosphere is of importance in optimizing the adaptive secondary control algorithm. To that end, a program of wavefront measurements at the telescope has been initiated. Since the telescope is not yet equipped with a secondary mirror, a small instrument has been constructed for deployment at the prime focus. The instrument package contains an imaging camera for point-spread function analysis, a finder camera, and a wavefront sensor almost identical to the production unit for the AO system. Results are reported in detail elsewhere in these proceedings;[4] they indicate close correspondence with the Kolmogorov spectrum.

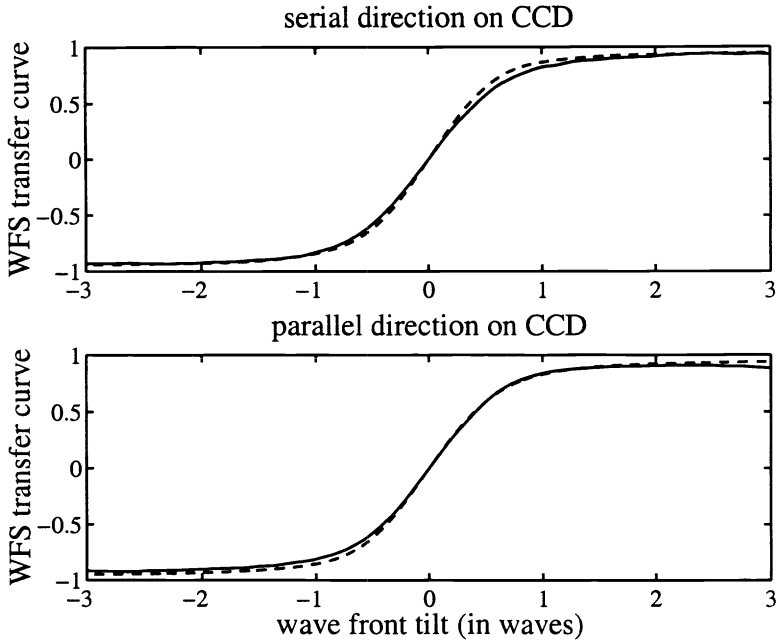

Figure 5. Measured transfer curves for the WFS. The solid lines are the measured data, and the dashed lines are predictions made on the basis of measured pixel cross-talk.

3.3. Adaptive Secondary

The design and integration of the secondary mirror control system is under contract with Media Lario, Lecco, Italy. The optical components, glass shell and reference plate, for both a sub-scale prototype and the full size unit were designed, fabricated and polished by the Steward Observatory Mirror Lab.

3.3.1. Prototype status

The thin shell mirror and the reference plate for the prototype were completed and delivered to Media Lario in early May 1999. The 36 actuator prototype, designated P36, has recently completed successful full speed dynamic tests at the Osservatorio Astrofisco di Arcetri in Florence,[3] marking the first time that a large, curved, continuous facesheet mirror has tracked a rapidly evolving Kolmogorov wavefront. The error in the tracking, as measured by the capacitive sensors associated with each actuator, is substantially smaller than the fitting error that would be expected from the high-frequency atmospheric aberration. In a closed-loop AO system therefore, mirror performance would not limit overall system performance.

3.3.2. The 336 actuator secondary

The reference plate (figure 6) and a spherical version of the full-scale thin shell mirror were completed and delivered to Media Lario in September 1999. Integration of the mechanical support and cooling system is now almost complete. Addition of the completed electronic assemblies and the actuators will then be followed by dynamic tests very similar to those carried out already on P36. After delivery of the secondary to Tucson, expected in early summer, the aspheric shell will be substituted for the sphere.

3.3.3 Thermal management

The secondary will dissipate about 2 kW, a value that is somewhat seeing-dependent. This waste heat must be removed, keeping the entire assembly as close to ambient temperature as possible. The actuators themselves are expected to generate about 250 W, which will be carried along the aluminum body of each actuator to a common cold plate (figure 7) and dumped into recirculating fluid. The driver electronics dissipate the bulk of the power, and they are contained in three insulated crates with cooling provided by the same fluid flow. Under normal seeing conditions, no part of the system's surface area will deviate from ambient temperature by more than ±2 °C.

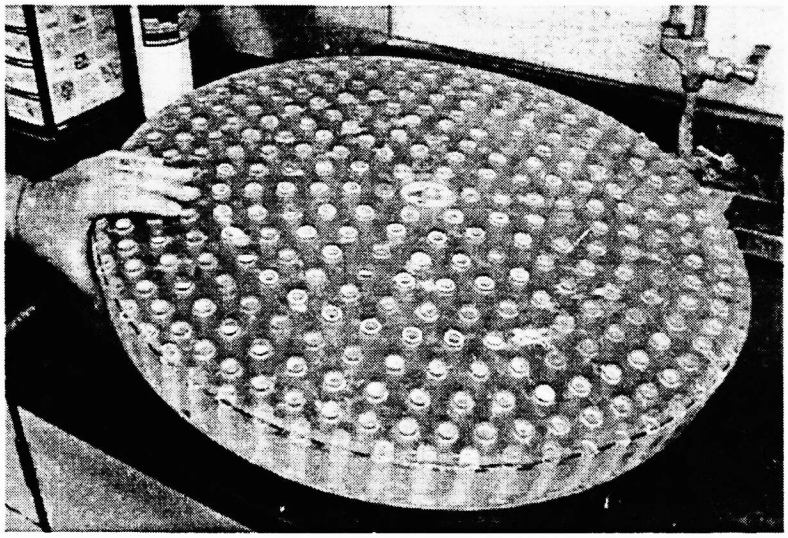

Figure 6. Glass reference plate for the adaptive secondary. The actuators project through the 336 holes piercing the plate. The thin mirror itself will be supported by the actuators above the top surface of this plate with a gap of 40 μm.

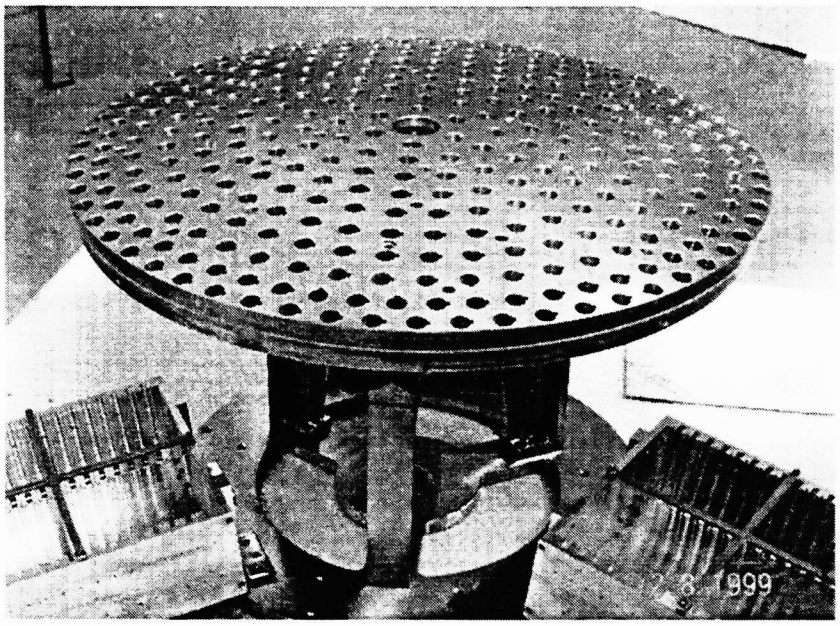

Figure 7. The cold plate for the 336 actuator adaptive secondary. The actuators mount in the holes, projecting radially toward the shell. The reference body shown in figure 6 mates to the top side of this plate, which is shown inverted with respect to its normal orientation in the telescope. Two of the three electronics crates appear at the bottom of the picture. They are hinged, and are shown here in their open position, without the cards installed.

3.4. System Control

The AO system is controlled from a TCL/Tk interface running on a PC under Linux. From there, over an ethernet connection, the user is able to issue commands to the real-time reconstructor machine and the alignment motors. In future, communication with the science instrument and the telescope itself will be added.

The wavefront reconstructor is hosted in a VME environment, and consists of a massively parallel matrix multiplier, with data routing handled by Texas Instruments C40 DSPs. Control of the electro-mechanical alignment systems is via a PC running Windows NT which communicates with different intelligent sensors and actuators via a CAN field-bus implementing the Device-Net protocol.[8]

4. MIRROR LAB TEST RESULTS

To date, although without the adaptive secondary we are unable to close the outer control loop, reconstructions from WFS data have shown good agreement with independent measurements recorded by the PSI. Figure 8 illustrates the correspondence for the case where no turbulence plate has been used, and only small alignment errors in the shimmulator optics remain.

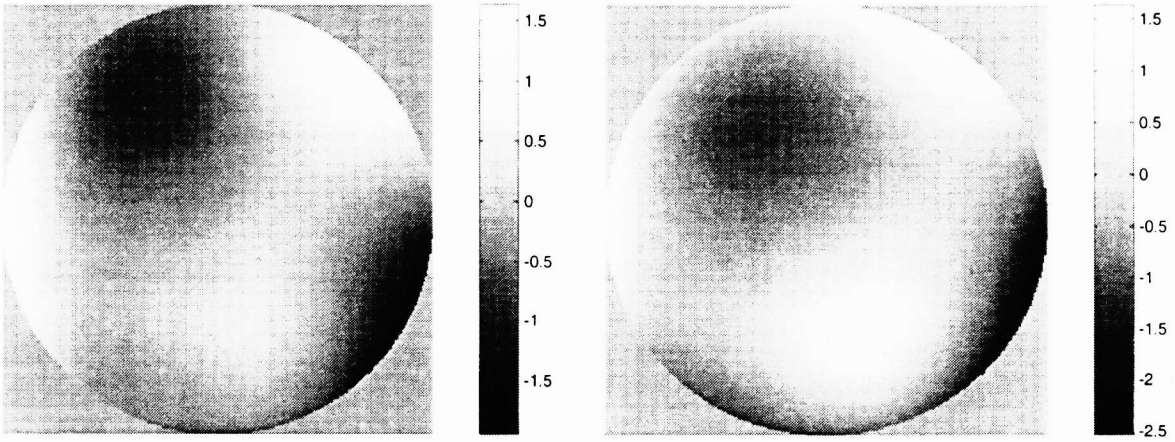

Figure 8. At left is a phase map recorded by the PSI installed as an integral part of the top box. The agreement with the phase reconstruction from the WFS at right is excellent.

To confirm that the statistics of the simulated turbulence are a reasonable match to what is expected at the telescope, and to give some confidence in the phase reconstructions from the WFS data, we have computed the spatial structure function from 128 reconstructed wavefronts. The result shown in figure 9 is a power law of index 1.80 and $D/r_0 = 17.3$. This closely corresponds to the statistics of the phase machined into the turbulence plates.[9]

ACKNOWLEDGEMENTS

We are grateful to the technical staff of both Steward Observatory and the MMTO for participating in this work. Thanks to Maud Langlois for providing Figure 1. The work has been supported by the Air Force Office of Scientific Research under grant numbers F49620-96-1-0366 and F49620-99-1-0285. The MMT is a joint facility of The University of Arizona and the Smithsonian Institution.

REFERENCES

1. C. Franchini, R. Biasi, & D. Gallieni, "MMT conversion adaptive secondary construction," these proceedings.
2. H. M. Martin et al., "Optical fabrication of the MMT adaptive secondary mirror," these proceedings.
3. A. Riccardi et al., "Adaptive secondary mirror for the 6.5 m conversion of the Multiple Mirror Telescope: final laboratory testing results of the P36 prototype," these proceedings.

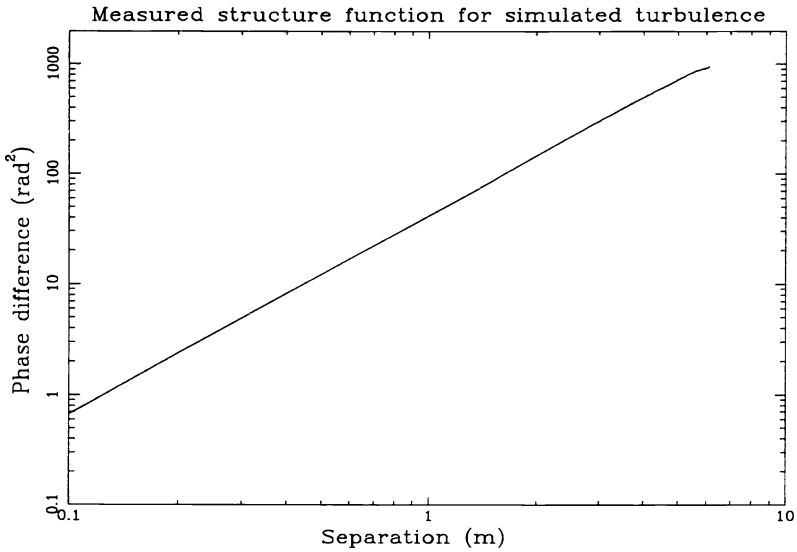

Figure 9. Spatial structure function of phase maps reconstructed from WFS data recorded in the shimmulator. The phase plates providing artificial turbulence give an excellent approximation to Kolmogorov seeing. The plotted separation is as projected onto the primary mirror.

4. P. C. McGuire et al., "Wavefront sensor measurements of atmospheric turbulence at prime focus of the new MMT," these proceedings.

5. J. T. Williams, C. B. Foltz, & S. C. West, "Commissioning of the 6.5-m MMT," *Telescope Structures, Enclosures, Controls, Assembly/Integration/Validation, and Commissioning* (Proc. SPIE), ed. T. A. Sebring & T. Andersen, **4004**, 2000.

6. M. Langlois, R. Angel, & M. Lloyd-Hart, "Prime focus coma corrector for the MMT with 'off the shelf' components," *Optical and IR Telescope Instrumentation and Detectors* (Proc. SPIE), ed. M. Iye & A. F. Moorwood, **4008**, 2000.

7. D. W. McCarthy, J. H. Burge, J. R. P. Angel, J. Ge, and B. C. Fitz-Patrick, "ARIES: Arizona infrared imager and echelle spectrograph," *Infrared Astronomical Instrumentation* (Proc. SPIE), ed. A. M. Fowler, **3354**, 1998.

8. G. Z. Angeli, B. C. Fitz-Patrick, M. Lloyd-Hart, & J. R. P. Angel, "Design and realization of ancillary control loops for the MMT adaptive optics system," *Telescope Structures, Enclosures, Controls, Assembly/Integration/Validation, and Commissioning* (Proc. SPIE), ed. T. A. Sebring & T. Andersen, **4004**, 2000.

9. T. A. Rhoadarmer, "Construction and testing of components for the 6.5 m MMT adaptive optics system," PhD thesis, University of Arizona, 1998.